

MAHMOOD AKBARI¹

ADSORPTION OF MCl_2 ($M = Hg, Cd, AND Pb$) ON $CuS(001)$ SURFACE. DENSITY FUNCTIONAL THEORY STUDY

We explored the adsorption properties of common heavy metal dichlorides ($HgCl_2$, $PbCl_2$, and $CdCl_2$) on the $CuS(001)$ surface using density functional theory (DFT) calculations. The most stable configuration of CuS was found the $CuS(001)$ surface, characterized by $Cu-S$ and $S-S$ terminations. We found that the adsorption energies on the $CuS(001)$ surface with $Cu-S$ termination are ordered as $HgCl_2 < CdCl_2 < PbCl_2$. Conversely, for the $CuS(001)$ surface with $S-S$ termination, the sequence is $HgCl_2 < PbCl_2 < CdCl_2$. This investigation into the adsorbate–surface interactions suggests that CuS is a promising candidate for the adsorption of these heavy metal molecules.

1. INTRODUCTION

Mercury, recognized as a toxic metal and hazardous air pollutant, poses significant health risks. During coal combustion in coal-fired power plants, mercury is vaporized into its elemental gaseous form, raising substantial environmental concerns. Besides elemental mercury, mercury dichloride ($HgCl_2$) emerges as another predominant form in flue gas, notorious for its acute and chronic toxicity [1–5]. Similarly, semi-volatile metals like lead and cadmium undergo partial evaporation in the furnace. The combustion or gasification of coal or biomass leads to the formation of heavy metal chlorides such as $PbCl_2$ and $CdCl_2$, which present challenges in efficient removal [6–10]. In response, recent research has pivoted towards mineral sulfides, particularly copper sulfide (CuS), as promising candidates surpassing traditional activated carbons for mercury removal. This is attributed to the sulfur active sites in mineral sulfides that facilitate mercury capture [11, 12].

Theoretical simulations offer invaluable insights into the adsorption processes of these complex species, especially where experimental verification is challenging [13–16]. This

¹UNESCO-UNISA-ITL Africa Chair in Nanoscience and Nanotechnology (U2ACN2), College of Graduate Studies, University of South Africa (UNISA), Pretoria, South Africa, email address: mahmoa@unisa.ac.za

study delves into the mechanisms underlying the capture of heavy metal dichlorides (MCl_2 , where M represents Hg, Cd, and Pb) by CuS, employing density functional theory (DFT). Our findings reveal a spectrum of interactions from weak to strong chemisorption on CuS surfaces, enhancing our understanding of the adsorption mechanism. This theoretical exploration not only complements experimental efforts but also broadens the scope for predicting and interpreting real-world applications.

2. COMPUTATIONAL DETAILS

Theoretical research demonstrates that the most stable surface of CuS is CuS(001) with Cu–S and S–S termination [17]. Hence, the CuS(001)/Cu–S (S1) and CuS(001)/S–S (S2) surfaces were constructed from the hexagonal bulk CuS with space group $P6_3/mmc$ with $a = b = 3.797 \text{ \AA}$ and $c = 16.441 \text{ \AA}$. A 4-layer slab with (3×3) unit cell and 12 \AA of vacuum in z -direction was used to model the surface structure. The position of all atoms except the atoms in the last two bottom layers of the surface was allowed to relax during the structure optimization. All calculations were performed in the framework of spin-polarized density functional theory (DFT) using the Perdew–Burke–Erzerhoff generalized gradient approximation (GGA-PBE) exchange-correlation functional [18], including Grimme-D3 dispersion correction [19, 20] applied in the Quantum-Espresso package [21]. The first Brillouin zone was modeled by a Monkhorst–Pack grid of gamma points only [22].

The adsorption E_{ads} of Hg, $HgCl_2$, $CdCl_2$, and $PbCl_2$ on two CuS(001) surfaces was studied, and the following expression calculates the adsorption energy

$$E_{\text{ads}} = E_{\text{slab} + \text{adsorbate}} - E_{\text{slab}} - E_{\text{adsorbate}} \quad (1)$$

The relative values of the Lowdin charges can help to determine the type of formed bond. Positive and negative values of the bond population, for example, indicate that the atoms are bonded or antibonded, respectively. A significant positive value indicates that the bond is mainly covalent, whereas a bond population close to zero indicates no interaction between the two atoms. We calculate the charge transfer ΔQ between the slab and adsorbent using the formula:

$$\Delta Q = Q_{\text{after}} - Q_{\text{before}} \quad (2)$$

being the difference of the adsorbent's charge after and before adsorption.

3. RESULTS AND DISCUSSIONS

This study utilized density functional theory (DFT) optimization at the B3LYP/lanl2dz level via Gaussian software [23] to analyze the gas-phase molecular structures of $HgCl_2$,

CdCl_2 , and PbCl_2 . HgCl_2 and CdCl_2 were identified as linear triatomic molecules with bond angles of 180° and bond lengths of 2.44 \AA and 2.37 \AA , respectively, facilitating their potential adsorption in both horizontal and vertical orientations on surfaces. In contrast, PbCl_2 exhibited a bent configuration with a Cl-Pb-Cl angle of 102° and bond lengths of 2.50 \AA .

Exploring various adsorption scenarios revealed that the most energetically favorable interactions with $\text{CuS}(001)$ surfaces – specifically, Cu-S (S1) and S-S (S2) sites – are illustrated in Figs. 1 and 2. Elemental Hg's interaction served as a benchmark for comparison.

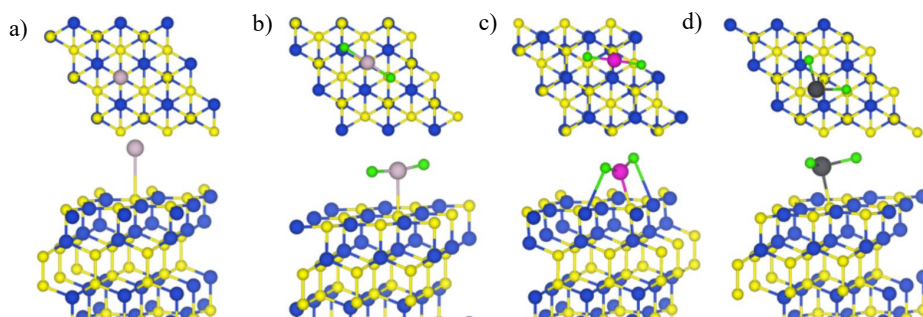


Fig. 1. The optimized configuration of Hg (a), HgCl_2 (b), CdCl_2 (c), and PbCl_2 (d) adsorbed on $\text{CuS}(001)$ surface with Cu-S termination (S1). Cu atoms are represented in blue, S atoms in yellow, Hg atoms in light violet, Cl atoms in green, Cd atoms in red, and Pb atoms in dark brown

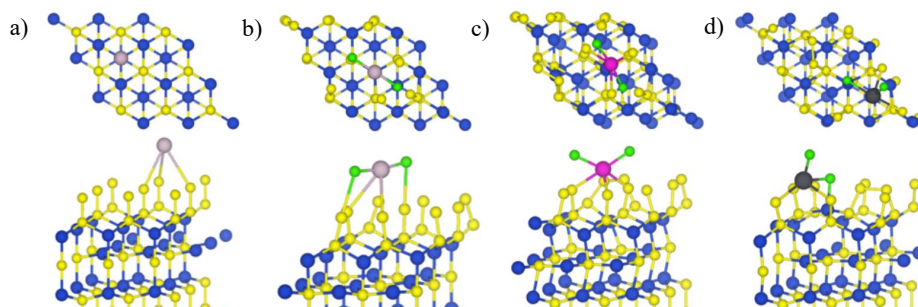


Fig. 2. The optimized configuration of Hg (a), HgCl_2 (b), CdCl_2 (c), and PbCl_2 (d) adsorbed on $\text{CuS}(001)$ surface with S-S termination (S2). Cu atoms are represented in blue, S atoms in yellow, Hg atoms in light violet, Cl atoms in green, Cd atoms in red, and Pb atoms in dark brown

Detailed analysis of data from Table 1 shows that HgCl_2 prefers a horizontal orientation at the S1 site, characterized by the adsorption energy of -0.44 eV and minimal charge transfer of 0.014 e , indicative of weak chemisorption. This configuration slightly alters the Cl-Hg-Cl angle to 171° . Conversely, a stronger interaction is observed at the

S2 surface, as noted in Table 2, where the adsorption energy deepens to -0.51 eV and charge transfer increases to -0.031 e, adjusting the molecule's angle to 170.5° .

Table 1

Optimized adsorption parameters of MCl_2 adsorbed on $CuS(001)$ surface with Cu-S termination (S1)

| Species | E_{ads} [eV] | $R_{M-Cu/S}$ [Å] | $\theta_{Cl-M-Cl}$ | | ΔQ [e] |
|-------------------|-------------------|---------------------|--------------------|------------------|-------------------|
| | | | Before adsorption | After adsorption | |
| Hg | -0.25 | 4.06 | – | – | – |
| HgCl ₂ | -0.44 | 3.25 | 179.93 | 171.00 | 0.014 |
| CdCl ₂ | -0.89 | 2.80 | 179.95 | 148.14 | 0.093 |
| PbCl ₂ | -0.90 | 3.02 | 101.56 | 99.50 | 0.270 |

E_{ads} is the adsorption energy calculated from Eq. (1), $R_{M-Cu/S}$ is the distance between the heavy metal atom (M) and the CuS surface, $\theta_{Cl-M-Cl}$ is the angle between the bond of metal dichlorides before and after adsorption, ΔQ is the charge transfer, [e] is the unit of elemental charge.

Table 2

Optimized adsorption parameters of MCl_2 adsorbed on $CuS(001)$ surface with S-S termination (S2)

| Species | E_{ads} [eV] | $R_{M-Cu/S}$ [Å] | $\theta_{Cl-M-Cl}$ | | ΔQ [e] |
|-------------------|-------------------|---------------------|--------------------|------------------|-------------------|
| | | | Before adsorption | After adsorption | |
| Hg | -0.21 | 3.96 | – | – | – |
| HgCl ₂ | -0.51 | 3.70 | 179.93 | 170.47 | -0.031 |
| CdCl ₂ | -1.93 | 2.60 | 179.95 | 121.17 | 0.039 |
| PbCl ₂ | -1.83 | 2.80 | 101.56 | 101.82 | 0.303 |

Symbols as in Table 1.

For $CdCl_2$, Table 1 indicates the most stable adsorption on the S1 surface (shown in Fig. 1c) characterized by weak chemisorption with an energy of -0.89 eV and a charge transfer of 0.093 e. In contrast, its interaction with the S2 surface intensifies significantly, as detailed in Table 2, with an interaction energy of -1.93 eV and a charge transfer of 0.039 e, indicative of strong chemisorption (Fig. 2c). The adsorption process induces bending of the molecule, reducing the Cl-Cd-Cl angle to 148.14° on S1 and further to 121.17° on S2.

Tables 1 and 2 reveal intriguing behaviors of $PbCl_2$'s adsorption, with Figs. 1d and 2d showcasing its most stable configurations on S1 and S2 surfaces, respectively. On S1, the molecule exhibits an adsorption energy of -0.90 eV and a notable charge transfer of 0.270 e, slightly altering the Cl-Pb-Cl angle to 99.50° . The strongest chemisorption is observed on S2, where the binding energy reaches -1.83 eV and the charge transfer peaks at 0.303 e, affirming the molecule's significant affinity and structural adaptation upon adsorption.

These findings not only elucidate the preferred adsorption configurations and energies of these toxic metal chlorides on CuS surfaces but also underscore the variability

in interaction strength and molecular geometry adjustments, offering deeper insights into the surface adsorption phenomena.

4. CONCLUSION

In conclusion, this comprehensive study has advanced our understanding of the interaction mechanisms between hazardous metal chlorides ($HgCl_2$, $CdCl_2$, and $PbCl_2$) and copper sulfide (CuS) surfaces through detailed density functional theory (DFT) analysis. Our findings underscore the potential of CuS as a superior adsorbent for mitigating pollution from toxic metals, a critical concern in coal combustion processes. The variations in adsorption energies and configurations for $HgCl_2$, $CdCl_2$, and $PbCl_2$ on CuS surfaces highlight the complexity of these interactions, ranging from weak to strong chemisorption. Notably, the study reveals how the molecular structure influences adsorption potential, with the linear molecules of $HgCl_2$ and $CdCl_2$ and the bent configuration of $PbCl_2$ displaying distinct adsorption behaviors and efficiencies.

This work not only provides a theoretical basis for the efficacy of CuS in capturing hazardous metal chlorides but also lays the groundwork for future experimental validations and applications. By elucidating the adsorption mechanisms at the molecular level, our research paves the way for developing more effective pollution control strategies, especially in coal-fired power plants where mercury and other semi-volatile metals pose significant environmental and health risks. Ultimately, these insights contribute to the broader pursuit of cleaner energy production and environmental preservation, underscoring the importance of innovative solutions in addressing the challenges of air pollution and heavy metal toxicity.

ACKNOWLEDGMENTS

The authors would like to thank the UNESCO-UNISA-ITL/NRF Africa Chair in Nanosciences and Nanotechnology (U2ACN2), and the Centre for High-Performance Computing (CHPC), South Africa, for this research project's computational resources and facilities.

REFERENCES

- [1] PACYNA E.G., PACYNA J.M., STEENHUISEN F., WILSON S., *Global anthropogenic mercury emission inventory for 2000*, Atmos. Environ., 2006, 40 (22), 4048–4063. DOI: 10.1016/j.atmosenv.2006.03.041.
- [2] YANG J., ZHAO Y., GUO X., LI H., ZHANG J., ZHENG C., *Removal of elemental mercury from flue gas by recyclable $CuCl_2$ modified magnetospheres from fly ash. Part 4. Performance of sorbent injection in an entrained flow reactor system*, Fuel, 2018, 220, 403–411. DOI: 10.1016/j.fuel.2018.01.132.
- [3] LI H., WU C.-Y., YING LI Y., ZHANG J., *CeO_2 - TiO_2 catalysts for catalytic oxidation of elemental mercury in low-rank coal combustion flue gas*, Environ. Sci. Technol., 2011, 45, 17, 7394–7400. DOI: 10.1021/es2007808.

- [4] ZOU S., LIAO Y., XIONG S., HUANG N., GENG Y., YANG S., *H₂S-modified Fe–Ti spinel: A recyclable magnetic sorbent for recovering gaseous elemental mercury from flue gas as a Co-benefit of wet electrostatic precipitators*, Environ. Sci. Technol., 2017, 51 (6), 3426–3434. DOI: 10.1021/acs.est.6b05765.
- [5] YANG J., ZHAO Y., ZHANG S., LIU H., CHANG L., MA S., ZHANG J., ZHENG C., *Mercury removal from flue gas by magnetospheres present in fly ash: Role of iron species and modification by HF*, Fuel Proc. Technol., 2017, 167, 263–270. DOI: 10.1016/j.fuproc.2017.07.016.
- [6] LIU S., WANG Y., YU L., OAKEY J., *Thermodynamic equilibrium study of trace element transformation during underground coal gasification*, Fuel Proc. Technol., 2006, 87 (3), 209–215. DOI: 10.1016/j.fuproc.2005.07.006.
- [7] FURIMSKY E., *Characterization of trace element emissions from coal combustion by equilibrium calculations*, Fuel Proc. Technol., 2000, 63 (1), 29–44. DOI: 10.1016/S0378-3820(99)00067-3.
- [8] GLAZER M.P., KHAN N.A., DE JONG W., SPLIETHOFF H., SCHÜRSMANN H., MONKHOUSE P., *Alkali metals in circulating fluidized bed combustion of biomass and coal: Measurements and chemical equilibrium analysis*, Energy Fuels, 2005, 19 (5), 1889–1897. DOI: 10.1021/ef0500336.
- [9] XU M., YAN R., ZHENG C., QIAO Y., HAN J., SHENG C., *Status of trace element emission in a coal combustion process: A review*, Fuel Proc. Technol., 2004, 85 (2–3), 215–237. DOI: 10.1016/S0378-3820(03)00174-7.
- [10] LINAK W.P., WENDT J.O.L., *Toxic metal emissions from incineration: Mechanisms and control*, Prog. Energy Combust. Sci., 1993, 19 (2), 145–185. DOI: 10.1016/0360-1285(93)90014-6.
- [11] LI H., ZHU L., WANG J., LI L., SHIH K., *Development of nano-sulfide sorbent for efficient removal of elemental mercury from coal combustion fuel gas*, Environ. Sci. Technol., 2016, 50, 17, 9551–9557. DOI: 10.1021/acs.est.6b02115.
- [12] WELEGERGS G.G., NUMAN N., DUBE S., NURU Z., BOTHA N., AZIZI S., CLOETE K., AKBARI M., MORAD R., TSEGAY M.G., GEBRETINSAE H., MTSHALI C., KHUMALO S., EZEMA F.I., KRIEF A., GIBAUD A., HENINI M., SEOPELA M.P., CHAKER M., MAAZA M., *Room temperature surface bio-sulfurisation via natural *sativum annilin* and bioengineering of nanostructured CuS/Cu₂S*, Nano-Horizons: J. Nanosci. Nanotechnol., 2023, 2. DOI: 10.25159/NanoHorizons.45486dad4f94.
- [13] KANAANI A., AKBARI M., VAKILI M., MORAD R., AJLOO D., MAAZA M., *Transition metals doped ZnS nanocluster for carbon monoxide detection: A DFT study*, Mater. Today Commun., 2023, 34, 105491. DOI: 10.1016/j.mtcomm.2023.105491.
- [14] MORAD R., AKBARI M., MAAZA M., *Theoretical study of chemical reactivity descriptors of some repurposed drugs for COVID-19*, MRS Advances, 2023, 8 (11), 656–660. DOI: 10.1557/s43580-023-00590-6.
- [15] AKBARI M., MORAD R., MAAZA M., *Effect of silver nanoparticle size on interaction with artemisinin: first principle study*, Res. Surf. Interf., 2023, 11, 100104. DOI: 10.1016/j.rsufi.2023.100104.
- [16] VAKILI M., KHEIRABADI R., AKBARI M., MORAD R., MAAZA M., *Computational studies of chalcogen doped on graphene vs. chalcogen doped on CNT and their role in the catalytic performance of electrochemical CO₂ reduction*, Mater. Today Commun., 2023, 35, 105631. DOI: 10.1016/j.mtcomm.2023.105631.
- [17] MORALES-GARCÍA A., HE J., SOARES A.L., DUARTE H.A., *Surfaces and morphologies of covellite (CuS) nanoparticles by means of ab initio atomistic thermodynamics*, CrystEngComm, 2017, 19, 3078–3084. DOI: 10.1039/C7CE00203C.
- [18] PERDEW J.P., BURKE K., ERNZERHOF M., *Generalized gradient approximation made simple*, Phys. Rev. Lett., 1996, 77, 3865. DOI: 10.1103/PhysRevLett.77.3865.
- [19] GRIMME S., ANTONY J., EHRLICH S., KRIEG H., *A consistent and accurate ab initio parametrization of density functional dispersion correction (DFT-D) for the 94 elements H–Pu*, J. Chem. Phys., 2010, 132, 154104. DOI: 10.1063/1.3382344.
- [20] GRIMME S., EHRLICH S., GOERIGK L., *Effect of the damping function in dispersion corrected density functional theory*, J. Comput. Chem., 2011, 32, 1456. DOI: 10.1002/jcc.21759.

- [21] SCANDOLO S., GIANNOZZI P., CAVAZZONI C., DE GIRONCOLI S., PASQUARELLO A., BARONI S., *First-principles codes for computational crystallography in the Quantum-ESPRESSO package*, *Z. Kristallogr. Cryst. Mater.*, 2009, 220 (5–6). DOI: 10.1524/zkri.220.5.574.65062.
- [22] MONKHORST H.J., PACK J.D., *Special points for Brillouin-zone integrations*, *Phys. Rev. B*, 1976, 13, 5188. DOI: 10.1103/PhysRevB.13.5188.
- [23] FRISCH M.J., TRUCKS G.W., SCHLEGEL H.B. et al., *Gaussian 16, Revision B.01*, Gaussian Inc., Wallingford, CT, 2016.